

Image engineering analysis using vascular structure parameters of peritumoral microvascular for radiosensitization effects on radiotherapy for malignant tumors

Tadataka Miyake, DDS (1), Hisashi Inami, DDS, PhD (2), Ryota Kawamata, DDS, PhD (2), and Takashi Sakurai, DDS, PhD (2)

(1) Tsurumi Dental Clinic, Yokohama, and (2) Division of Radiopraxis Science, Department of Maxillofacial Function Reconstruction, Kanagawa Dental University, Yokosuka, Japan

Purpose: This study evaluated the effects of combination therapy by *in vivo* experiment under conditions closely resembling actual clinical cancer treatment. The relationship between therapeutic efficacy and peritumoral microvascular structure changes was also evaluated with image-engineering analysis.

Materials and Methods: Fifty 8-week-old female BALB/cAJcl-nu/nu mice were used as humanoid tumor models. Five experimental groups were set; control, radiotherapy, thermoradiotherapy, chemoradiotherapy, and thermochemoradiotherapy. The therapeutic effect was evaluated based on tumor volume ratios before and after treatment, vascular structure parameters on magnified angiographic X-ray images, and histopathological examination.

Results: Tumor volume ratios in all treatment groups were significantly lower than in the control group. Magnified angiographic X-ray images showed that peritumoral vessels were decreased in each treatment group. Each combination therapy group showed further reductions and fragmentations compared with the radiotherapy group. In quantitative analysis of extracted vascular structure patterns, the reduction in blood vessels with radiotherapy was slight, thermoradiotherapy achieved strong reductions and reduced continuity and caused fragmentation, and chemoradiotherapy and thermochemoradiotherapy achieved more marked reductions and fragmentation. In histopathological evaluations, many viable tumor cells remained following radiotherapy. In contrast, viable tumor cells completely disappeared with each combination therapy.

Conclusion: These findings suggest that radiotherapy in combination with hyperthermia and chemotherapy achieves high antitumor efficacy, and triple-combination therapy will reduce the burden on patients. Furthermore, these experimental results suggest that the stronger the therapeutic effect of the combination therapy, the more peritumoral blood vessels will be reduced and fragmented.

(Asian Pac J Dent 2016; 16: 35-46.)

Key Words: Chemotherapy, Hyperthermia, Image engineering analysis, Oncology, Radiotherapy

Introduction

Different therapies used for the treatment of malignant tumors have differing characteristics. For example, surgery for malignant tumors is not appropriate for patients who cannot tolerate severe invasive treatment due to systemic factors or who lack the basic physical strength to withstand the surgery. Furthermore, in the case of surgery, since surrounding normal tissue must also be excised in consideration of the risk of small, residual lesions, tumor invasion, and lymph node metastasis, esthetic and functional effects of the tissue defects associated with lesion resection have the potential to significantly reduce the quality of life of patients [1].

In contrast, conservative treatment methods such as anticancer chemotherapy and radiotherapy have the potential to inhibit malignant tumor growth and eliminate malignant tumors while maximizing the preservation of healthy tissues, without the invasiveness of surgery [2-5]. However, therapeutic efficacy is not always certain with those treatments, and sufficient therapeutic effect sometimes cannot be obtained. There is also a risk of serious disorders resulting from these therapies. To obtain more reliable therapeutic effects within a short time period using conservative treatments, various combination therapies have been applied to take advantage of the benefits of each, and the results of various such combination therapies have been reported [2-9].

We have previously reported an *in vitro* study using the human KB cell line, derived from an epidermal carcinoma of the mouth, to investigate the sensitizing effects of various combinations of radiotherapy,

chemotherapy using a taxoid antineoplastic agent, and thermotherapy [10]. Those results suggested that even with dosages showing almost no efficacy when used alone, the combination of these three treatments showed very potent cytotoxicity, suggesting the possibility of good therapeutic efficacy. However, the *in vivo* therapeutic effects of treatments can be greatly impacted by changes in the microcirculation caused by the blood flow changes that accompany the growth and treatment of tumors. Therefore, even if a treatment shows strong cytotoxic effects *in vitro*, that treatment may not result in similar therapeutic efficacy *in vivo*.

To date, *in vivo* studies relating to radiotherapy have been flawed in that they have been carried out under conditions far removed from those used for actual clinical radiotherapy regimens, such as employment of only a single, high dose of irradiation or high-dose hypofractionated irradiations, representing a serious flaw [11-14]. This is because clinical therapeutic effects cannot be accurately assessed from cases of single, high-dose irradiation or high-dose hypofractionated irradiation.

The objective of this study was to establish noninvasive combination therapy with good therapeutic effect for reducing the prescription dosage and shortening treatment duration. This study confirmed the effects of combination therapy indicative of excellent treatment effects in our past *in vitro* study, by *in vivo* experiment under conditions closely resembling actual clinical cancer treatment. We also performed image-engineering analysis of therapy-induced changes in the peritumoral microvascular structure to elucidate the relationship between these changes and therapeutic efficacy.

Materials and Methods

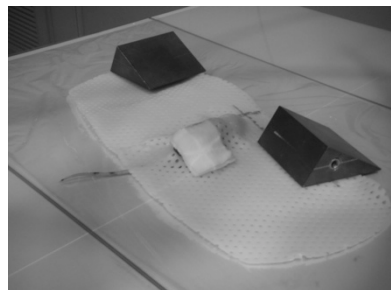
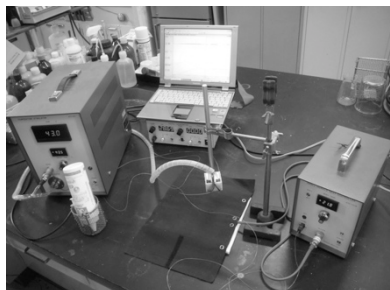
Experimental animal and cell line

Humanoid tumor model mice were made using athymic mice and human KB cells. Fifty 8-week-old female BALB/cAJcl-nu/nu mice (Clea Japan Inc. Ltd., Tokyo, Japan) were used, with 10 animals in each experimental group. In this study, a control group and four experimental groups for radiotherapy (RT), thermoradiotherapy (RT+HT), chemoradiotherapy (RT+CH), and thermochemoradiotherapy (RT+HT+CH) were set. Human KB cells (Japanese Collection of Research Bioresources Cell Bank, Osaka, Japan), derived from an epidermal carcinoma of the mouth, were inoculated subcutaneously at a dose of 5×10^6 cells to prepare a mouse model of humanoid tumor. Treatment of the animals was started four weeks after KB cell inoculation, and therapeutic effects were assessed one week after treatment completion. Due to the loss of animals to death, etc., analysis during the treatment period was performed for three animals in each group for which the final efficacy assessment had been successfully performed. Long- and short-axis diameters of tumors were measured at the start of treatment and at the time of efficacy assessment. Tumor volumes were calculated before and after treatment using the following formula: $\pi/6 \times \text{long-axis diameter} \times \text{short-axis diameter}^2$. The change in tumor volume from before to after treatment was evaluated using the equation: tumor volume ratio = post-treatment volume/pretreatment volume. All experiments were carried out in accordance with Japanese national animal protection laws and our institutional guidelines for the care and handling of experimental animals (institutional approval number 2007-56).

Treatment

Radiotherapy (RT): Tumors were irradiated with 6-MV X-rays using a linear accelerator radiotherapy system (HL-1500; Hitachi Medical Co. Ltd., Tokyo, Japan). Each tumor was exposed to X-rays at a dose rate of 1.8 Gy/min, 2 Gy/fraction, 1 fraction/day, 5 days/week, with a source-to-tumor distance of 100 cm. The total

absorbed dose was set at 70 Gy. Each mouse was immobilized using an immobilization shell without anesthesia, and irradiation was performed. Figure 1 shows the state of a representative mouse during RT. Depth from the surface to the center of the tumor was adjusted using moistened gauze on the surface of the immobilization shell, to make the percentage depth dose 100% at the predicted center of the tumor under X-ray irradiation.

**Fig. 1****Fig. 1** Status at the time of irradiation for mice**Fig. 2****Fig. 2** The heating and temperature monitoring system constructed for the purpose of thermotherapy for small animals**Fig. 3****Fig. 3** Status at the time of thermotherapy for mice

Thermoradiotherapy (RT+HT): RT+HT was performed using a regimen that has been applied clinically in Japan. That is, RT was administered five times a week, preceded on the first of those occasions each week by local HT at 43°C for 30 min. The total absorbed X-ray dose was set at 70 Gy, and RT was combined with HT a total of seven times during the treatment period. Radiation conditions were otherwise the same as those used for RT alone. Figure 2 shows the heating and temperature-monitoring system constructed for the purpose of HT for small animals. A small-animal heating and cooling controller (BTC-201; Unique Medical Co., Ltd., Tokyo, Japan) connected to a custom-built 3-cm-diameter heating probe was used for local hyperthermia. To prevent temperature decreases due to heat dissipation on the table side, a small-animal heat controller (ATC-101B; Unique Medical Co., Ltd.) was placed between the animal and the experimental table. Control of the intratumoral temperature during warming was achieved by monitoring the heating probe temperature, skin surface temperature, and rectal temperature throughout treatment. In addition, correlations between intratumoral temperature and heating probe temperature, skin surface temperature, and rectal temperature were confirmed in a preliminary experiment to decide the heating conditions required to achieve an intratumoral temperature of 43°C. Temperatures were measured using a portable digital thermometer (PTW-301; Unique Medical Co., Ltd.; temperature error range $\pm 0.2^\circ\text{C}$). At the time of HT, each mouse was placed under general anesthesia by intraperitoneal injection of 50 mg/kg of sodium pentobarbital (Kyorin Pharmaceutical Co., Ltd., Tokyo, Japan). Figure 3 shows the set-up during HT for mice.

Chemoradiotherapy (RT+CH): Docetaxel (Taxotere; Sanofi-Aventis, Paris, France), a taxane that inhibits microtubule depolymerization, was used for CH. In consideration of the dosage at which this agent is employed in clinical settings in Japan, docetaxel was administered at 60 mg/m^2 as a caudal vein injection 30 min before irradiation. For each mouse, body surface area in square centimeters was calculated from body weight in grams using the following formula described by DuBois: body surface area (cm^2) = $96.47 + 1.577 \times \text{body weight (g)}$. As in the case of RT+HT, CH was administered once a week at the first of the five weekly irradiation treatments, and was coadministered a total of seven times during the course of administration of the total RT dose of 70 Gy.

Thermochemoradiotherapy (RT+HT+CH)

Irradiation conditions were the same as those for the other therapies, with HT and CH both coadministered once weekly with one of the five weekly RT treatments. Conditions for docetaxel administration were the same as those for RT+CH, and HT was performed 30 min after docetaxel administration under the same conditions as for RT+HT. Irradiation was performed immediately after the completion of HT. For this triple-combination therapy, the total absorbed dose of radiation was set at 32 Gy, and coadministration with both HT and CH was performed a total of three times during the treatment period.

Evaluation of vascular structures

Vascular structures surrounding the tumor were evaluated one week after the completion of treatment. For that evaluation, we applied a non-destructive quantitative analysis based on magnified angiographic X-ray images that we have reported previously [15]. During angiography, each mouse was placed under general anesthesia by intraperitoneal injection of sodium pentobarbital at 50 mg/kg (Sumitomo Dainippon Pharma Co. Ltd., Osaka, Japan). An indwelling catheter was placed in the aorta by thoracotomy, and 1.0 mL of barium sulfate (150 w/v%; Kaigen Pharma Co., Ltd., Osaka, Japan) was injected intra-arterially. Immediately after injection, X-ray magnification imaging was performed using a microfocus tube X-ray imaging system (P70-II; Pony Atomic Industry Co., Ltd., Tokyo, Japan) and computed radiography system (FCR-5000MA; Fuji Photo Film Co., Ltd., Tokyo, Japan). Exposure conditions were as follows: tube voltage, 30 kV; tube current, 90 μ A; exposure time, 10 s; focus-to-objective distance, 4.7 cm; and focus-to-imaging plate distance, 33 cm with 7 times magnification. Mice were positioned in the abdominal position and exposed to X-rays by anteroposterior projection.

A region of interest of 350×350 pixels was set at the tumor site on magnified angiographic X-ray images, and a mathematical morphological filter was used for extraction of the vascular structure pattern. The mathematical morphological filter was applied using a skeleton operation equation and a single disk-shaped structuring element with a diameter of five pixels. In this study, vascular structure pattern images of sum-set n = 2-5 were extracted for evaluation and the extracted vascular structure pattern images were binarized at a threshold level of 1. These binarized image data were then used for quantitative analysis. Image analysis software (Bone version 1.3; Idea Garden Co., Ltd., Tokyo, Japan) was used for quantitative analysis of the vascular structure pattern. The following seven parameters were evaluated as vascular structure parameters in this study: blood vessel area (BV.A); blood vessel peripheral length (BV.P); blood vessel peripheral length/blood vessel area (BV.P/BV.A); blood vessel number (BV.N); blood vessel volume (BV.V); nodule number (N.Nd); and blood vessel length with continuity/ total blood vessel length (Nd.Nd/TBL).

Histopathological evaluations

When animals were sacrificed, peritumoral tissue specimens were fixed in 4% paraformaldehyde phosphate buffer (Wako Pure Chemical Industries, Ltd., Osaka, Japan) and thin sections of 4 μ m thickness were prepared. Sections were stained with hematoxylin and eosin in accordance with the usual method and histologically evaluated under light microscopy (BX51TF; Olympus Corporation, Tokyo, Japan).

Statistical analyses

Statview version 5.0 software (SAS Institute Inc., NC, USA) was used for all statistical analyses. Dunnett's test was used for comparisons between control and experimental groups, while the Tukey-Kramer test was used for comparisons between experimental groups. Values of $P < 0.05$ were taken to indicate a statistically significant difference.

Results

Tumor volume ratio

Figure 4 shows examples of tumor state in representative mice from each experimental group before and after treatment. Figure 5 depicts tumor volume ratio for each experimental group before and after treatment. In the control group, tumor volume ratio reached 7.4 during the eight-week observation period. The tumor volume ratio of the RT group was 3.4, significantly lower than the value in the control group. The ratio of the RT+HT group was 2.4, even lower than in the RT group. Tumors showed marked reductions in size in the RT+CH group and RT+HT+CH group, and tumors had almost disappeared on macroscopic examination after treatment. In all treatment groups, tumor volume ratio was significantly smaller compared with the control group.

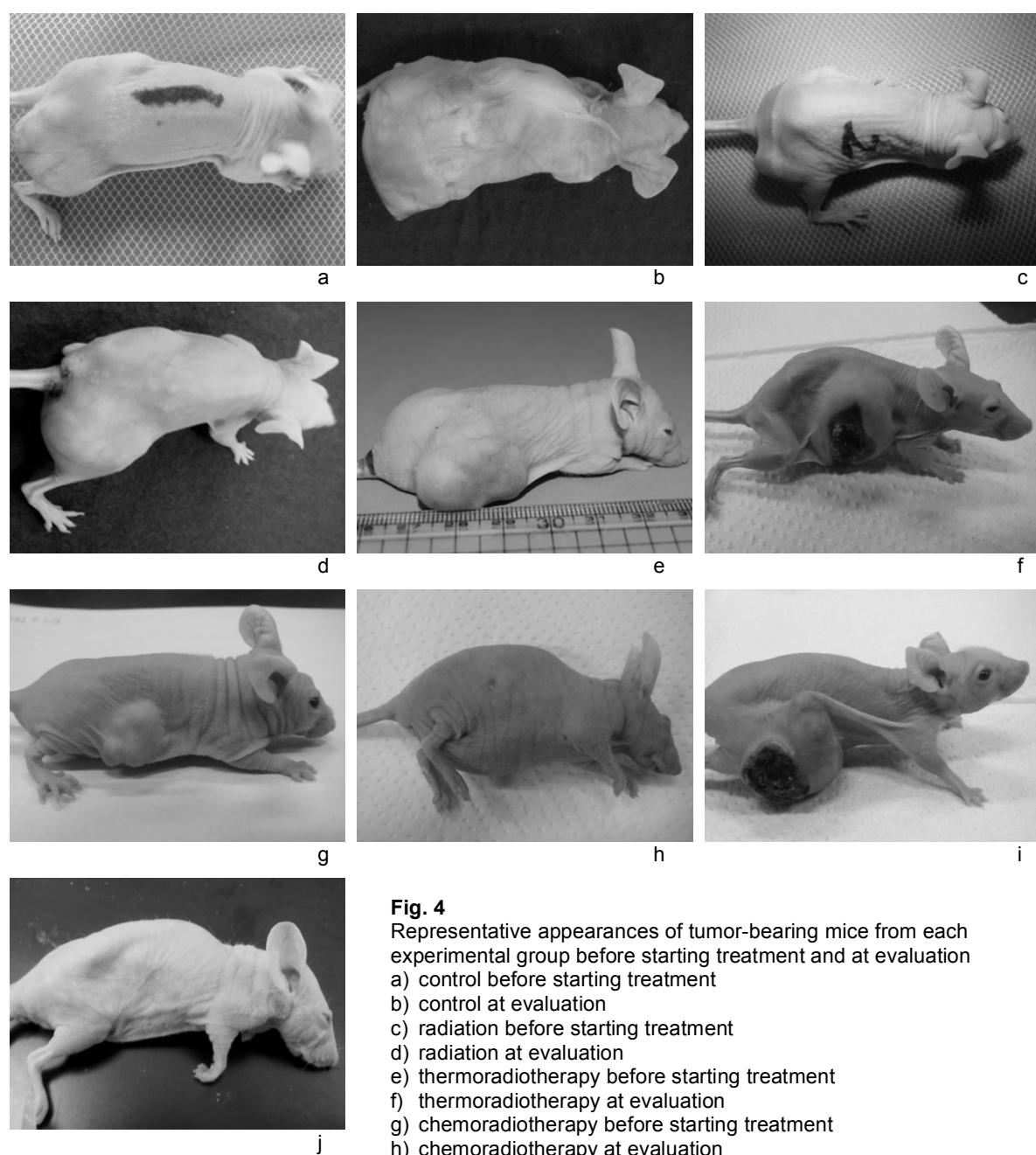


Fig. 4

Representative appearances of tumor-bearing mice from each experimental group before starting treatment and at evaluation

- a) control before starting treatment
- b) control at evaluation
- c) radiation before starting treatment
- d) radiation at evaluation
- e) thermoradiotherapy before starting treatment
- f) thermoradiotherapy at evaluation
- g) chemoradiotherapy before starting treatment
- h) chemoradiotherapy at evaluation
- i) thermochemoradiotherapy before starting treatment
- j) thermochemoradiotherapy at evaluation

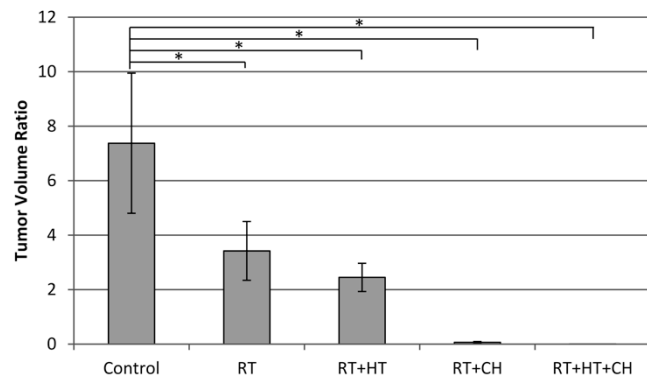
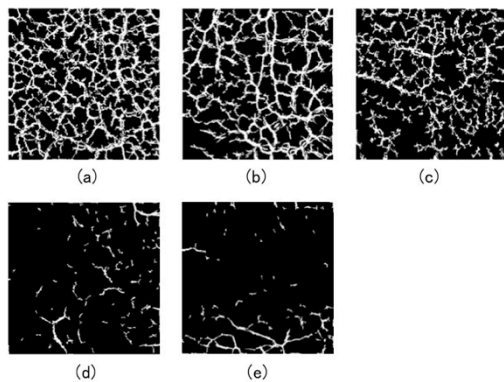
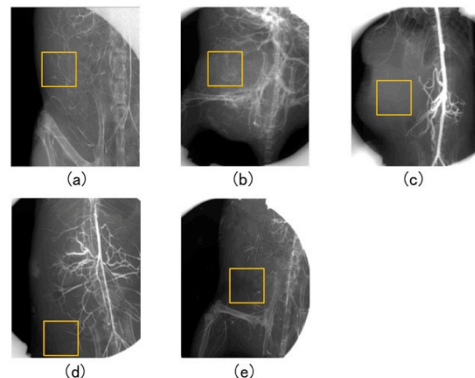
**Fig. 5****Fig. 7****Fig. 6**

Fig. 5 Tumor volume ratio for each experimental group before starting treatment and at evaluation. Vertical bars indicate ± 1 standard deviation (SD). * $P < 0.05$

Fig. 6 Magnified angiographic images in the vicinity of the tumor from each experimental group at the time of evaluation. Squares show the region of interest for mathematical morphological filter processing and quantitative evaluation. **a)** control; **b)** radiotherapy; **c)** thermoradiotherapy; **d)** chemoradiotherapy; **e)** thermochemoradiotherapy

Fig. 7 Examples of vascular structure patterns extracted using with the mathematical morphological filter for each experimental group after treatment. **a)** control; **b)** radiotherapy; **c)** thermoradiotherapy; **d)** chemoradiotherapy; **e)** thermochemoradiotherapy

Evaluation of vascular structure

Figure 6 shows magnified angiographic X-ray images and Fig. 7 shows extracted vascular structure patterns processed using the mathematical morphological filter for each experimental group. Visual qualitative assessment confirmed that peritumoral vessels in each treatment group were decreased compared to the control group. In addition, each combination therapy group showed further reductions in blood vessels compared with the RT group, and fragmentation was confirmed.

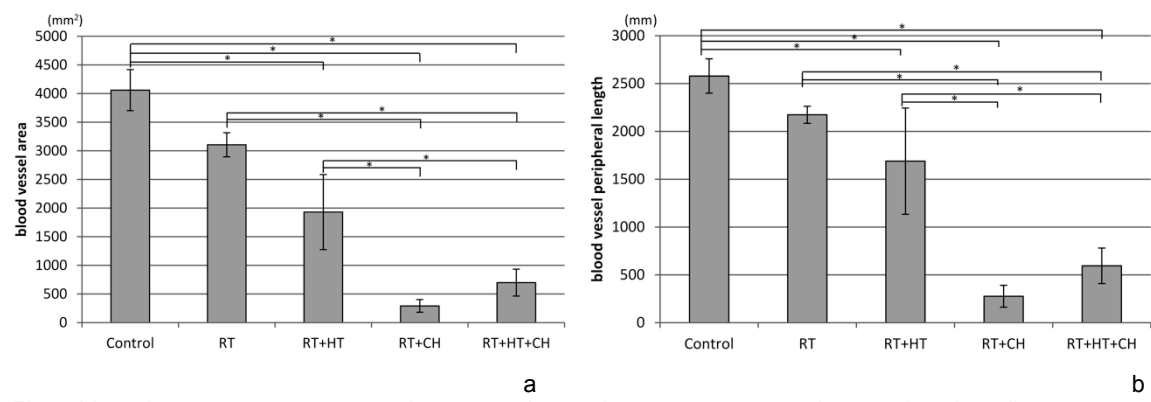
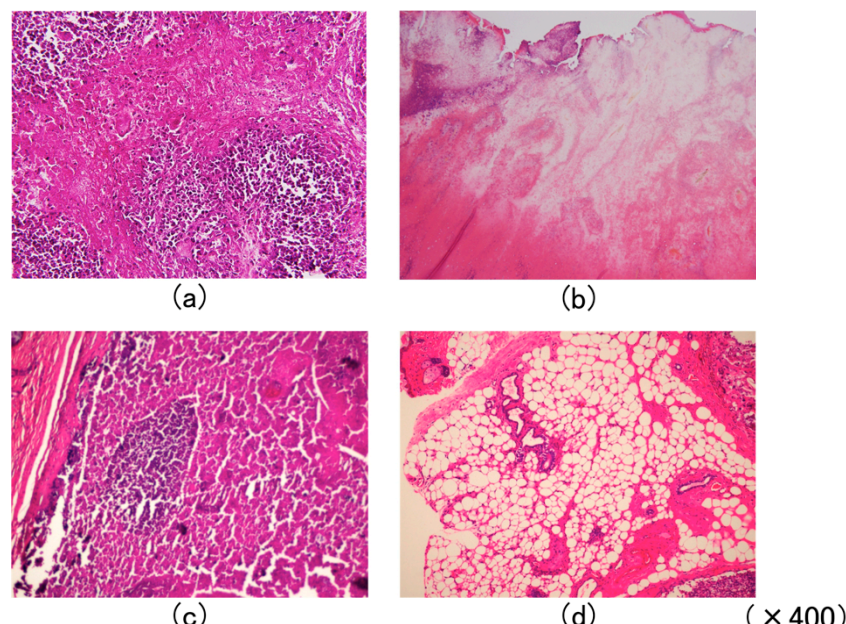
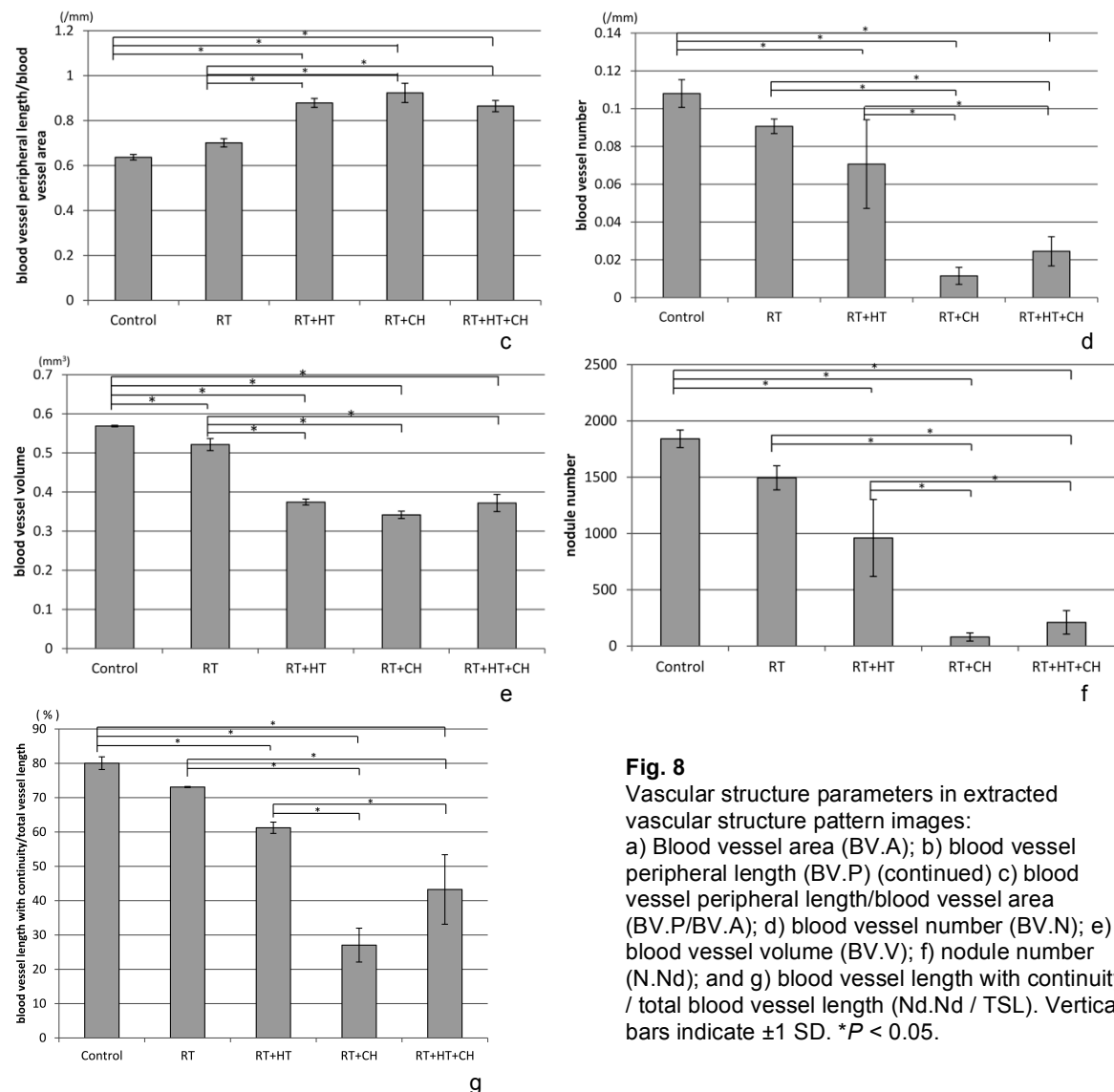
**Fig. 8** Vascular structure parameters in extracted vascular structure pattern images (continued)

Figure 8 shows the results of quantitative analysis of extracted vascular structure patterns. For BV.A (Fig. 8a), the RT group did not show any significant difference compared with the control group, but values were significantly lower in the other treatment groups than in the control group. In addition, although the difference between the RT and RT+HT groups was not significant, BV.A was significantly lower in the RT+CH and RT+HT+CH groups than in the RT and RT+HT groups. Results for BV.P (Fig. 8b) resembled those for BV.A.



The BV.P/BV.A ratio (Fig. 8c), did not differ significantly between control and RT groups, but was significantly higher in each of the three combination therapy groups (RT+HT, RT+CH, and RT+HT+CH) compared with both the control and RT groups. However, unlike the cases of BV.A and BV.P, no significant differences were seen among the three combination therapy groups. Results for BV.N (Fig. 8d) were similar to those for BV.A and BV.P, with no significant differences between control and RT groups, but significantly lower BV.N was observed in each of the three combination therapy groups (RT+HT, RT+CH, and RT+HT+CH) than in the control group. Moreover, although no significant difference was found between the RT and RT+HT groups, the RT+CH and RT+HT+CH groups each showed a significantly lower BV.N than the RT and RT+HT groups. All treatment groups showed significantly lower BV.V than the control group (Fig. 8e). While each combination therapy group showed a significantly lower BV.V than the RT group, no significant differences were seen among combination therapy groups. Results for N.Nd (Fig. 8f) and Nd.Nd/TSL (Fig. 8g) were similar to the results for BV.A, BV.P, and BV.N. Quantitative analysis of these parameters revealed the following. The RT group differed significantly from the control group only in regard to BV.V, with no other parameters showing any significant differences. The reduction in blood vessels with RT was thus slight. Each of the three combination therapy groups (RT+HT, RT+CH, and RT+HT+CH) showed significantly lower BV.A, BV.P, BV.N, and BV.V values compared with the control group, indicating that combination therapies achieved strong reductions in blood vessels. At the same time, each combination therapy group showed elevation of BV.P/BV.A and reduction of N.Nd and Nd.Nd/TSL. Those findings reveal that combination therapies reduced the continuity of blood vessels and caused fragmentation. Furthermore, compared with the RT+HT group, the RT+CH and RT+HT+CH groups showed even lower values of BV.A, BV.P, BV.N, N.Nd, and Nd.Nd/TSL. Those findings indicate that compared with RT+HT, use of RT+CH and RT+HT+CH brought about more marked blood vessel reduction and fragmentation.

Histopathological evaluations

Figure 9 shows representative histopathological findings after the completion of treatments. In the RT group, about half of the tumor cells in the tumor were seen to have undergone necrosis, but many viable tumor cells remained. In the RT+HT group, viable tumor cells had completely disappeared, and the lesion displayed hyaline-like degeneration with strong lymphocyte infiltration seen around the degenerated lesion. In the RT+CH group, tumor cells had completely disappeared and only a necrotic lesion was observed. Likewise in the RT+HT+CH group, absolutely no residual tumor cells were seen, and adipose-like degenerative tissue was evident at the tumor site.

Discussion

RT using X-rays achieves efficacy primarily through the direct effects of ionizing radiation and the indirect effects of free radical formation *in vivo* [16]. The sensitivity to radiation differs with the histological type of the tumor, but even for tumors of the same histological type, radiation sensitivity is decreased by decreases in the blood flow supplying the central region of the tissue as the tumor tissue grows. These decreases in blood flow cause decreases in both the intratumoral partial pressure of oxygen and pH, in turn reducing the sensitivity to radiation. This process has been elucidated as the reason sufficient therapeutic effects are often not obtained around the central portion of tumor tissues [17].

The present study indicated that RT alone achieved a certain degree of inhibition of tumor growth, but

histopathological examinations revealed regions with numerous viable tumor cells remaining inside the tumors. Although X-ray microangiography of the RT-alone group showed slight decreases in the number of blood vessels compared with the control group, an interconnected vascular structure was maintained. Although the results of vascular structure analysis of the same image revealed that BV.V was significantly reduced, indicating a reduced volume of peritumoral microvessels, other parameters for the vascular structure did not show any significant differences. Such findings indicate that continuity of the vascular structure was preserved and suggest that the blood supply was maintained in the case of RT alone. Thus, because the treatment effects of RT alone are limited in terms of cytological, biological, and molecular biological results, various multimodal therapies, including combination with surgery, are applied for the treatment of lesions such as severely advanced or metastatic cancers [2-9]. With the combination of RT and HT, the HT acts effectively in tumor tissues under conditions of low oxygen and low pH, which reduce radiation sensitivity, and the heat also inhibits repair of the genetic damage caused by ionizing radiation, thereby amplifying radiation sensitivity. Moreover, HT and RT act synergistically, because cells show high sensitivity to HT in the S phase of the cell cycle, which increases cell resistance to radiation [4]. Kurpeshev et al. compared RT alone to RT+HT in the treatment of locally advanced oral cancer and reported significant differences in the complete response rate and time to local recurrence when HT was combined with conventional RT, and noted that the combination of RT and HT might contribute to better local tumor control and long-term survival [18].

In the present study, combination of HT with RT further reduced the tumor volume ratio compare with RT alone, and histopathological examination revealed no viable tumor cells. Vascular structure pattern images showed very fine blood vessels remaining in the tumor tissue, but with poor continuity and evident fragmentation. Quantitative analysis of the same images showed that compared with radiation alone, BV.V was significantly lower and BV.P/BV.A was significantly higher. In the case of RT+HT, these results suggest that the reduction in the number of blood vessels is slight, but the fragmentation of vascular structures is increased. Based on those findings, fine vascular structures throughout the tumor tissue appear to be disrupted when temperature increases with the addition of HT. Then, in the vicinity of sites that are directly heated, tumor cells disappear concomitant with a strong inflammatory response, and stronger therapeutic effects can be thought to result compared with radiation alone accompanied by degeneration.

In the case of CH, drugs delivered via the circulation are intended to eliminate tumor tissues through cytotoxicity. For that reason, even if tumor tissues are not overly sensitivity to radiation, chemotherapeutic agents are able to achieve therapeutic efficacy proportional to the blood flow to the tumor tissue [19]. In particular, squamous cell carcinomas of the head and neck region are highly likely to be accompanied by metastases from the primary tumor to cervical lymph nodes, and marked neogenesis of feeding blood vessels is seen [20]. As methods of drug administration for combined RT and CH to lesions in the head and neck region, many cases treated by super-selective intra-arterial infusion of CH via the femoral artery or superficial temporal artery have been reported [21,22]. Currently, representative chemotherapeutic agents to treat head and neck tumors include docetaxel, cisplatin, and 5-fluorouracil, and many reports have described the use of multidrug regimens [22].

Among those drugs, docetaxel expresses antitumor activity by inhibiting microtubule depolymerization and thus causing cell cycle arrest. Since this agent prolongs the highly radiosensitive G2 and M phases, the radiosensitivity of tumor cells in RT+CH is also elevated. An *in vivo* study by Mason et al. showed that the

therapeutic ratio could be improved by devising an administration schedule for docetaxel and RT irrespective of whether tumor cells were docetaxel-resistant, and they suggested that RT+CH with docetaxel represented a useful treatment for advanced, inoperable head and neck cancers [23]. Similarly, histopathological findings for the RT+CH group in the present study showed complete necrosis of the tumors, with no observable viable tumor cells. Vessels extracted from vascular structure pattern images were markedly reduced in number, and the network structure had been fragmented. Quantitative analysis also revealed that the RT+CH group showed significant differences in each parameter compared with the control and radiation-only groups, suggesting that the local circulation had been severely affected by combination of treatment.

The prognosis is poor for patients with advanced, inoperable head and neck cancers, especially stage III and IV cases, and various multimodal protocols have been used in attempts to prolong survival [21,22,24-27]. Case reports of triple-combination therapy employing RT, CH, and HT have shown better results than cases treated with combination therapy using two modalities. Itazawa et al. employed RT+CH in combination with HT to treat 11 patients with locally advanced head and neck cancer and bulky cervical lymph node metastasis [24]. They reported complete response in eight patients, partial response in two patients, and no change in one patient, for a 90.9% response rate, and 1- and 2-year survival rates of 90.9 % and 42.4 %, respectively. Mitsudo et al. treated cases of oral cavity squamous cell carcinoma with N2 or N3 cervical lymph node metastasis by administration of triple-combination therapy comprising retrograde super-selective intra-arterial infusion CH using both docetaxel and cisplatin, plus RT and HT [21]. They identified no uptake to cervical metastatic lymph nodes on post-treatment ¹⁸F-fluorodeoxyglucose positron emission tomography, and histopathological examination showed no presence of viable tumor cells. Those previous reports suggested that triple-combination therapies provided high clinical therapeutic efficacy. However, all patients who received RT were irradiated with an absorbed dose exceeding 50 Gy at the lesion center, and the risk of side effects from such high-dose radiation must be considered. Moreover, docetaxel is known to cause advanced bone marrow suppression as well as kidney and liver failure, and HT can injure the mucous membranes, skin, and surrounding tissues. Thus, even with the use of ordinary dosages for each component of multimodal therapy, caution is required with regard to the possibility of very serious side effects resulting from therapeutic interactions and synergies.

Based on this background, the present study was carried out using less than half the usual dosages for each component of the triple-combination therapy. The objective was to investigate the feasibility of reducing dosages in order to reduce both invasiveness and the risk of postoperative side effects, while achieving reliable therapeutic efficacy. The results showed marked decreases in blood vessel patterns on vascular structure pattern images, very few and sparse residual fragmented patterns in the tumors, and histopathological findings of complete elimination of tumor tissues accompanied by fatty degeneration. The results of quantitative analyses also showed significant reductions of blood vessels in the triple-combination therapy group compared with the control and RT-only groups. These findings suggested that sufficiently high therapeutic efficacy was obtained even when using less than half the usual dosages for each individual treatment modality.

This study, which used KB cells as a human oral squamous epithelium-derived malignant tumor line, suggests that RT in combination with HT and CH achieve high antitumor efficacy by reducing and fragmenting microvessels around the tumor. Furthermore, this triple-combination therapy enabled decreases in the dosages of each treatment modality to less than half that usually applied clinically, and appears likely to prove useful for shortening the duration of treatment and reducing the burden on patients. Our findings further suggest that the

stronger the therapeutic effect of combination therapy, the more peritumoral blood vessels will be reduced and fragmented. Further analyses are needed to optimize the prescribed combinations, timings, and dosages of the individual components in multimodal therapy, with the aim of minimizing both side effects and reductions in quality of life while achieving complete cure of patients.

Acknowledgements

The authors express our sincere thanks to Prof. Keiichi Tsukinoki, Division of Environmental Pathology, Department of Oral Science, for his thoughtful advice and pathological support regarding this work.

Conflict of interests

The authors declare that there is no conflict of interests regarding the publication of this paper.

References

1. Kamil H, Nelke, Wojciech P, Hanna G, Jaroslaw L. Head and neck cancer patients' quality of life. *Adv Clin Exp Med* 2014; 23: 1019-27.
2. Seagren SL. Recent advances in radiation therapy of head and neck cancer. *Head Neck Surg* 1982; 4: 227-32.
3. Maehara Y, Kuwano H, Kitamura K, Matsuda H, Sugimachi K. Hyperthermochemoradiotherapy for esophageal cancer. *Anticancer Res* 1992; 12: 805-10.
4. Rao W, Deng ZS, Liu J. A review of hyperthermia combined with radiotherapy/chemotherapy on malignant tumors. *Crit Rev Biomed Eng* 2010; 38: 101-16.
5. Day FL, Leong T, Ngan S, Thomas R, Jefford M, Zalcberg JR, et al. Phase I trial of docetaxel, cisplatin and concurrent radical radiotherapy in locally advanced oesophageal cancer. *Br J Cancer* 2011; 104: 265-71.
6. Goerner M, Seiwert TY, Sudhoff H. Molecular targeted therapies in head and neck cancer—an update of recent developments. *Head Neck Oncol* 2010; 2: 8.
7. Dillman RO. Cancer immunotherapy. *Cancer Biother Radiopharm* 2011; 26: 1-64.
8. Kolev M, Towner L, Donev R. Complement in cancer and cancer immunotherapy. *Arch Immunol Ther Exp* 2011; 59: 407-19.
9. Ca'ceres W, Cruz-Chaco'n A. Renal cell carcinoma: molecularly targeted therapy. *P R Health Sci J* 2011; 30: 73-7.
10. Sakurai T, Hara M, Kawamata R, Kozai Y, Innami H. A basic in vitro study on effective conservative combined therapy for malignant tumors. *Oral Radiol* 2012; 28: 48-54.
11. Julia AM, Bachaud JM, Canal P, Daly NJ. Radiosensitivity of jejunal mucosa after whole abdomen irradiation and CDDP pretreatment. *Int J Radiat Oncol Biol Phys* 1991; 20: 343-5.
12. Epperly MW, Goff JP, Franicola D, Hong W, Peter W, Song L, et al. Esophageal radioprotection by swallowed JP4-039/F15 in thoracic-irradiated mice with transgenic lung tumors. *In Vivo* 2014; 28: 435-40.
13. Filatenkov A, Baker J, Müller AM, Ahn GO, Holbrook K, Suparna D, et al. Treatment of 4T1 metastatic breast cancer with combined hypofractionated irradiation and autologous T-cell infusion. *Radiat Res* 2014; 182: 163-9.
14. Koonce NA, Quick CM, Hardee ME, Jamshidi-Parsian A, Dent JA, Paciotti GF, et al. Combination of gold nanoparticle-conjugated tumor necrosis factor- α and radiation therapy results in a synergistic antitumor response in murine carcinoma models. *Int J Radiat Oncol Biol Phys* 2015; 93: 588-96.
15. Sakurai T, Kawamata R, Kashima I. Development of a quantitative analysis method for measuring the change in vascular structure of malignant tumors in small experimental animals. *Oral Radiol* 2008; 24: 1-9.
16. Franklin H. Chemical changes in DNA by ionizing radiation. *Prog Nucleic Acid Res Mol Biol* 1985; 32: 115-54.
17. Brizel DM, Sibley GS, Prosnitz LR, Scher RL, Dewhirst MW. Tumor hypoxia adversely affects the prognosis of carcinoma of the head and neck. *Int J Radiat Oncol Biol Phys* 1997; 38: 285-9.
18. Kurpeshev OK, Ostapenko VV, Mardynsky YS, Chushkin NA. Retrospective analysis of therapy for locally advanced oral cancer: radiotherapy alone and thermoradiotherapy. *Thermal Med* 2009; 25: 59-70.
19. Seiwert TY, Salama JK, Vokes EE. The chemoradiation paradigm in head and neck cancer. *Nat Clin Pract Oncol* 2007; 4: 156-71.
20. Shah JP. Patterns of cervical lymph node metastasis from squamous carcinomas of the upper aerodigestive tract. *Am J Surg* 1990; 160: 405-9.
21. Mitsudo K, Koizumi T, Iida M, Mitsunaga S, Tohnai I. Thermochemoradiotherapy for oral cancer with N2, 3 cervical lymph node metastases using retrograde superselective intra-arterial infusion. *Thermal Med* 2012; 28: 23-8.
22. Kashiwagi N, Fujii T, Nishiyama K, Tomiyama N, Yagyu Y, Tsurusaki M, et al. Superselective intra-arterial chemotherapy with concurrent radiotherapy for advanced parotid squamous cell carcinoma: a case report. *Jpn F Clin Oncol* 2015; 45: 378-80.
23. Mason KA, Kishi K, Nunter N, Buchmiller L, Akimoto T, Komaki R, et al. Effect of Docetaxel on the therapeutic ratio of fractionated radiotherapy in vivo. *Clin Cancer Res* 1999; 5: 4191-8.
24. Itazawa T, Watai K, Kurihara S, Inoue T. Hyperthermia combined with chemoradiotherapy for treatment of locally advanced head and neck cancer with bulky lymph node metastasis. *J Hyperthermic Oncol* 2007; 22: 151-8.
25. Ang KK, Zhang Q, Rosenthal DI, Nguyen-Tan PF, Sherman EJ, Weber RS, et al. Randomized phase III trial of concurrent accelerated radiation plus cisplatin with or without cetuximab for stage III to IV head and neck carcinoma: RTOG 0522. *J Clin Oncol* 2014; 32: 2940-50.
26. Davis MA, Tyrrell J, Slotman GJ, Sudhindra R, Sachdeva K, Fanelle J, et al. Preoperative simultaneous fractionated cisplatin and radiation therapy in the treatment of advanced operative stage III and IV squamous cell carcinoma of the head and neck. *Am J Surg* 2015; 209: 575-9.
27. Inohara H, Takenaka Y, Yoshii T, Nakahara S, Yamamoto Y, Yomiyama Y, et al. Phase 2 study of docetaxel, cisplatin, and concurrent radiation for technically resectable stage III-IV squamous cell carcinoma of the head and neck. *Int J Radiat Oncol Biol Phys* 2015; 91: 934-41.

Correspondence to:

Dr. Hisashi Innami
Division of Radiopraxis Science, Department of maxillofacial function reconstruction,
Kanagawa Dental University
82 Inaoka-cho, Yokosuka 238-8580, Japan
Fax: +81-46-822-8850 E-mail: innami@kdu.ac.jp

Accepted October 11, 2016.

Copyright ©2016 by the *Asian Pacific Journal of Dentistry*.

Online ISSN 2185-3487, Print ISSN 2185-3479